


# Quantifying the effects of load carriage and fatigue under load on sacral kinematics during countermovement vertical jump with IMU-based method

Ryan S. McGinnis<sup>1</sup>  · Stephen M. Cain<sup>2</sup> · Steven P. Davidson<sup>3</sup> · Rachel V. Vitali<sup>2</sup> · Noel C. Perkins<sup>2</sup> · Scott G. McLean<sup>3</sup>

Published online: 14 October 2015  
© International Sports Engineering Association 2015

**Abstract** We present a method for quantifying sacral kinematics during countermovement jumping (CMJ) using an inertial measurement unit (IMU). The IMU-derived sacral kinematic trajectories reproduced motion capture acceleration, velocity, and displacement to within mean (standard deviation) differences of 0.024 (0.088) m/s<sup>2</sup>, 0.023 (0.026) m/s, and 0.003 (0.032) m, respectively, across 252 jumps performed by 14 subjects. The method also quantified differences in maximum sacral displacement to within 1 % and differences in maximum propulsive velocity to within 0.7 % of motion capture estimates. This builds upon existing IMU-based methods for quantifying jump performance, which do not provide sacral kinematic trajectories. The utility of this method is demonstrated by its ability to discriminate jump performance metrics across a diverse subject population. In particular, we found that 21 participants adopted multiple strategies to maximize jump height in unloaded and loaded fresh conditions, but converged to a common strategy when jumping fatigued and under load. Changes in kinematic parameters were evident across conditions, and several changes were significantly associated with changes in jump performance (i.e., height). These parameters include changes in the depth of the countermovement, duration of the propulsive phase and maximum propulsive velocity. Collectively, these results point toward the future use of

this method in naturalistic environments and for multiple objectives including biomechanical performance assessment and tracking, fatigue assessment, and jump training.

## 1 Introduction

Vertical jumping is paramount for success in sports including basketball, volleyball, and football where an athlete's ability to elevate his or her center of mass can be the difference between success and failure. Indicators of jumping technique have been identified from subject mass center kinematic trajectories [1, 2], which in turn point toward existing strength and technique deficits and enable focused training efforts to accelerate improvement. Beyond these applications, performance (i.e., jump height) in a countermovement vertical jump (CMJ) has been used as an indicator of lower body power [3, 4] which renders this simple task an effective screening tool to assess biomechanical capacity. As a result, performance in the CMJ has been used to track functional strength changes that result from training programs (e.g., see [5] for a study on strength changes due to military training) or rehabilitation [6], and has been used to inform return to play decisions [7]. Moreover, degradation in CMJ height has been established as an indicator of neuromuscular fatigue [8, 9], further suggesting that the CMJ could serve as a fatigue assessment tool. The potential use of CMJ for these applications (i.e., jump performance optimization, strength deficit identification, biomechanical performance assessment and tracking, and fatigue assessment) is challenged by measuring jump kinematics in naturalistic (non-laboratory) environments.

There are a number of existing measurement technologies for quantifying CMJ biomechanical performance. In

✉ Ryan S. McGinnis  
ryanmcg@umich.edu

<sup>1</sup> MC10, Inc., Cambridge, MA, USA

<sup>2</sup> Department of Mechanical Engineering, University of Michigan, Ann Arbor, MI, USA

<sup>3</sup> School of Kinesiology, University of Michigan, Ann Arbor, MI, USA

research contexts, optical motion capture (MOCAP) [10] and/or force plates [9, 11–15] ultimately quantify sacral or mass center kinematics and jump height. However, these technologies are not practical for use outside of a motion laboratory and therefore do not readily translate to the aforementioned applications. Similarly, a single high-speed video camera could be used to quantify sacral kinematics (as an analog to mass center kinematics) and height of the CMJ, but doing so requires a camera operator and post hoc video processing which again hinder translation. Also popular are jump stands [10, 16, 17], but they only quantify jump height and can be inaccurate relative to gold standard MOCAP [10]. Photoelectric systems [12, 13, 15, 18, 19] (i.e., Optojump, Microgate Corp., Bolzano, ITA) and contact mats [8, 10, 14–17, 20] (i.e., Just Jump System, Probotics Inc., Huntsville, AL, USA) estimate jump height based on flight time, but they remain bulky, require set-up time and post hoc data processing, and do not provide kinematic trajectories which limits their utility.

An attractive alternative to these measurement modalities are body-worn inertial sensors. Several studies have explored the use of accelerometers for quantifying jumping [1, 13, 17, 18, 21]. For example, a single-axis accelerometer has been used to quantify sacral acceleration during squat jumping, with jump height estimated via flight time [1]. However, doing so requires that the accelerometer sense axis remains vertical which precludes its use for the CMJ. The Myotest (Myotest SA, Sion, CHE) system, which utilizes a tri-axial accelerometer, has been validated against optoelectronic systems for calculating jump height [18] via flight time, but it also exhibited a clinically significant systematic bias in estimated flight time compared to force plate data [13]. Regardless, the Myotest system yields only an estimate of jump height and not complete sacral kinematics during the jumping motion.

Several studies improved upon the accelerometer-based methodologies by combining a tri-axial accelerometer with a tri-axial angular rate gyroscope, forming what is known as an inertial measurement unit (IMU) [11, 22, 23]. One study [11] employed a commercial IMU (Keimove device, Vincid, Granada, ESP) that provides estimates of take-off velocity and flight time, but does not otherwise provide jump height or sacral kinematics. Proprietary algorithms were used to estimate take-off velocity and flight time which preclude adaption to other IMU hardware and possibly to other types of jumps. For example, jumps with significant leg or torso motion in flight could potentially invalidate their estimates. In contrast, [23] presented a general algorithm for estimating countermovement jump height based on measurements from an IMU affixed to the lower back of a subject. The algorithm requires integration of the measured acceleration to yield estimates of take-off velocity and height, both of which are used to estimate

jump height via ballistic motion assumptions [23]. However, it is well established [24] that integration of measured acceleration introduces significant drift error in estimated velocity and position and [23] did not mention this potential error source. Drift error could reduce the accuracy of the estimated take-off velocity and height and therefore the calculated jump height. Moreover, this algorithm does not provide kinematic information during the jumping motion which limits its utility.

Extending this approach, we present a method for calculating sacral kinematics and CMJ height using a single IMU affixed to the sacrum. We establish the validity of this method by comparing against optical motion capture. Validation extends to conditions where CMJ performance is affected by load carriage and by fatigue. Doing so reveals key kinematical measures of CMJ performance that are sensitive to and discriminate between unloaded versus loaded and fresh versus fatigued conditions. These kinematical measures may also serve as CMJ performance metrics to support training and the identification of technique deficits.

## 2 Methods

### 2.1 Human subjects

For the validation study, 16 subjects (9 males aged  $23.4 \pm 4.6$  years, height  $180.7 \pm 8.7$  cm, mass  $79.7 \pm 15.8$  kg; 7 females aged  $26.1 \pm 6.9$  years, height  $168.7 \pm 4.4$  cm, mass  $65.7 \pm 6.8$  kg) were recruited from the local university population for participation. For the performance study, 21 subjects (15 males aged  $19.7 \pm 1.1$  years, height  $178.7 \pm 6.9$  cm, mass  $78.0 \pm 9.6$  kg; 6 females aged  $20.2 \pm 1.0$  years, height  $172.4 \pm 4.9$  cm, mass  $68.0 \pm 8.1$  kg) were recruited from the local ROTC programs for their experience exercising to fatigue under the load conditions considered in this experiment. Prior to testing, informed written consent was obtained from each participant and approval was obtained from the University of Michigan Institutional Review Board.

### 2.2 IMU hardware

The IMUs used in both parts of this study were YEI 3-Space sensors (Yost Engineering, Portsmouth, OH). These devices incorporate a MEMS accelerometer (3-axis) and angular rate gyro (3-axis) which provide direct measurement of the linear acceleration at the accelerometer and the angular velocity of the device, respectively. Prior to use, the IMUs were calibrated following the procedure detailed in [25]. Data were sampled at approximately 300 Hz, written to on-board flash memory, and

subsequently downloaded to a computer via USB after each subject's data collection session. The remainder of the Sect. 2 is presented in two parts, namely the Validation Task and Performance Task, to clearly describe the methods used for each.

### 2.3 Methods for validation task

To establish the validity of the proposed IMU-based method, IMU-derived kinematics were compared to MOCAP-derived kinematics during 20 CMJs (10 each in loaded and unloaded configurations), for each of 16 subjects. The 20 jumps consisted of four 5-jump trials, where load condition was randomly assigned. Subjects began standing still in a neutral posture, performed their CMJ with the goal of jumping as high as possible, returned to their neutral posture as quickly as possible after the jump, and then repeated this sequence at a self-selected pace for the five jumps in each trial. During these jumps, the IMU and attached marker frame (Fig. 1) were affixed to the pelvis of each subject and located as close to the sacrum as possible (midway between the left and right posterior superior iliac spine anatomical landmarks). Each subject was instructed to jump as high as possible while wearing

the US Army's Improved Outer Tactical Vest (IOTV) with Enhanced Small Arms Protective Insert (ESAPI) training plates and the Tactical Assault Panel (TAP) during the loaded condition and without the training plates or panel in the unloaded condition (Fig. 1). The difference in mass between loaded and unloaded conditions was approximately 18 kg. Subject noncompliance with the given instructions (i.e., subject's not returning to a neutral posture between jumps), MOCAP marker occlusion, and IMU malfunction precluded use of 68 jumps and yielded 252 jumps from 14 subjects for analysis as reported below.

#### 2.3.1 Sacral kinematics from optical motion capture

The three-dimensional (3D) position of four retro-reflective markers, 12 mm in diameter and affixed to the pelvic-mounted IMU marker frame (Fig. 1) were recorded at a frequency of 100 Hz using an 8-camera VICON optical motion capture system (VICON Motion Systems, Oxford, UK). Gaps in the raw marker trajectories produced by marker occlusion were identified and treated within the VICON Nexus software (VICON Motion Systems, Oxford, UK) using cubic spline interpolation.

For each sample, the location of the sacrum beneath the subject-worn IOTV was then approximated as the point in space where the distance between two lines, one fit to each pair of markers affixed to each leg of the marker frame, is minimized. Numerical differentiation of the vertical component of this sacral position yields vertical velocity and a second differentiation yields the vertical acceleration for comparison to their corresponding IMU-derived quantities as described next.

#### 2.3.2 Sacral kinematics from an inertial measurement unit

Calculation of the IMU-derived sacral kinematics begins by calculating the vertical acceleration of the sacrum. To this end, we introduce a body-fixed reference frame ( $B$ ) which is defined by the orthonormal triad ( $\hat{e}_1, \hat{e}_2, \hat{e}_3$ ) and is aligned with the sense axes of the IMU. Next, we introduce a ground-fixed reference frame ( $G$ ) defined by the orthonormal triad ( $\hat{E}_1, \hat{E}_2, \hat{E}_3$ ) where  $\hat{E}_1$  and  $\hat{E}_2$  are contained within the horizontal plane and  $\hat{E}_3$  is aligned with gravity. Given the accelerometer output from the IMU ( $\vec{a}_m$ ) resolved in frame  $B$ , we can write the IMU-estimated vertical acceleration of the sacrum ( $a$ ) as

$$a = (C_{G/B} \vec{a}_m - g \hat{E}_3) \cdot \hat{E}_3, \quad (1)$$

where  $g$  is the gravitational acceleration constant ( $9.81 \text{ m/s}^2$ ), and  $C_{G/B}$  is the direction cosine matrix that describes the orientation of the ground frame relative to the body frame determined via integration of the angular velocity following the method presented in [24]. Numerical

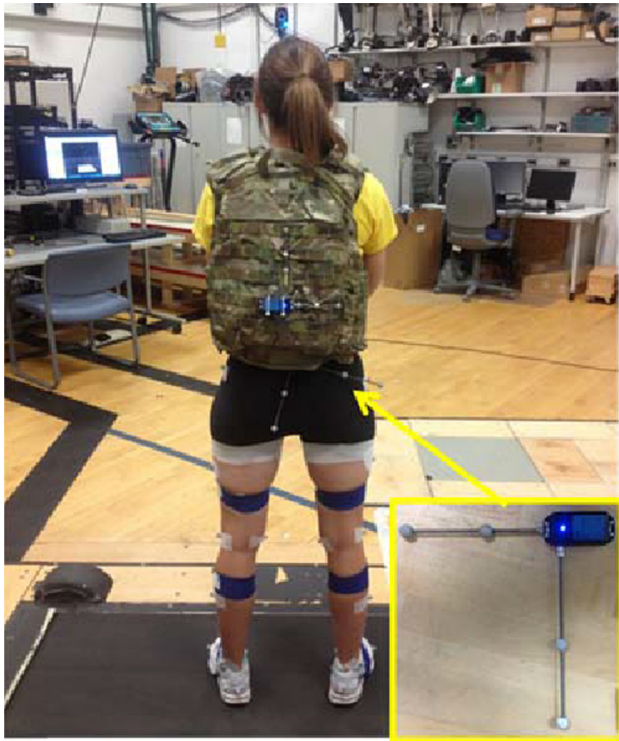


**Fig. 1** IMU and attached marker frame used for this study (callout) were indexed against the pelvis of each subject and affixed as close as possible to the sacrum, between the subject and their Improved Outer Tactical Vest (IOTV). A second IMU and marker frame is visible on the IOTV and used for a separate validation study

integration of the vertical acceleration yields an estimate of sacral vertical velocity ( $\tilde{v}$ ) polluted by drift error, which is a well-established phenomenon associated with inertial sensors [26, 27]. Approximately accounting for this drift, the corrected sacral vertical velocity ( $v$ ) is defined as a function of time ( $t$ ) per

$$v(t) = \tilde{v}(t) - (a_0 + a_1 t) \quad (2)$$

where  $(a_0 + a_1 t)$  is a linear approximation to the drift error in velocity. To identify the constants  $a_0$  and  $a_1$ , we exploit known end conditions on the sacral velocity of the subject; namely, that immediately before and after the CMJ the subject's sacrum is at rest. These two velocity conditions uniquely determine the two constants ( $a_0, a_1$ ) and thus the corrected vertical velocity of the subject over the duration of the jump. Similarly, numerical integration of the vertical velocity yields an estimate of the vertical displacement of the sacrum ( $\tilde{d}$ ) polluted by drift error. The drift-corrected sacral vertical displacement ( $d$ ) is defined as a function of time per

$$d(t) = \tilde{d}(t) - (b_0 + b_1 t), \quad (3)$$

where  $(b_0 + b_1 t)$  is a linear approximation to the drift error in displacement. Identifying the constants  $b_0$  and  $b_1$  in this case is not as straightforward as it was for Eq. (2) as the subject's sacral displacement after the jump is unknown. However, we know that before and after the jump the subject is still, and that after the jump the subject's sacrum has returned to a height that is close to its starting position (by instruction). With this in mind, we identify  $b_0$  and  $b_1$  such that the displacement before the jump is zero, and the following objective function is minimized

$$f = (\tilde{d}(t_e) - (b_0 + b_1 t_e))^2 + \left( \frac{d}{dt} \tilde{d}(t_e) - b_1 \right)^2 + \left( \frac{d}{dt} \tilde{d}(t_s) - b_1 \right)^2, \quad (4)$$

where  $t_s$  corresponds to a start time just prior to the jump and  $t_e$  corresponds to an end time immediately following the jump when the subject is still. Any constrained optimization technique (e.g., the method of Lagrange multipliers) can then be used to identify the constants  $b_0$  and  $b_1$  yielding a drift-corrected estimate of the sacral displacement over the duration of the jump.

MOCAP and IMU estimates of the sacral vertical acceleration, velocity, and displacement were each low-pass filtered at 15 Hz prior to comparison. Validity of the IMU kinematic trajectories were established by reporting mean (SD) differences between the two motion sensing modalities in addition to intercept, slope and  $R^2$  values for best-fit lines to correlation plot data. Validity of IMU-estimated jump height and maximum vertical velocity (two metrics often used to assess jump performance) is

established via Bland–Altman graphical analysis and by reporting mean (SD) differences between the two motion sensing modalities in addition to intercept, slope and  $R^2$  values for best-fit lines to correlation plot data. To establish concurrent validity of the IMU estimates, paired-sample  $t$  tests ( $\alpha = 0.05$ ) are used to test for significant changes in jump height, maximum vertical velocity, and maximum vertical acceleration across load in both the IMU and MOCAP data. In these comparisons, and throughout the remainder of the manuscript, jump height is defined as the maximum vertical displacement of the sacrum from its initial position while the subject is standing at rest prior to the jump. We consider this metric in particular because it provides direct indication of the bottom line performance (i.e., distance the subject propels herself off the ground).

## 2.4 Methods for performance task

After establishing the validity of the IMU-derived sacral kinematics, we proceed to investigate the effects of fatigue and load carriage on sacral kinematics during the CMJ. To this end, subjects were asked to complete repeated cycles of an obstacle course until fatigue was achieved. Similar to the validation tests, subject data were collected in both loaded (IOTV + ESAPI plates + TAP panel), and unloaded conditions (IOTV). The first cycle of the course was completed in the unloaded condition and all subsequent bouts were completed in the loaded condition. At the start of the unloaded and first loaded bouts, the subject performed four CMJs in succession at maximal effort. Results from the four loaded jumps were averaged and used to establish the subject-specific maximum jump height. Following these loaded jumps, subjects then completed repeated rounds of the obstacle course (designed to induce neuromuscular fatigue), each of which ended with four CMJs in succession at maximal effort. Immediately prior to each set of jumps, subject heart rate and perceived exertion (relative to the Borg's CR10 scale [28]) were recorded. Subject fatigue was identified by one of the following metrics: (1) heart rate reaching maximum heart rate (220-age in BPM) at the end of consecutive bouts; (2) perceived exertion reports of 10 at the end of consecutive bouts, or (3) vertical jump height dropping below 70 % of the subject's maximum value [8].

### 2.4.1 Instrumentation and kinematic parameterization

During the CMJ, subjects were instrumented with an IMU mounted to the pelvis (as close to the sacrum as possible) using a tightened nylon belt. The algorithms presented above were used to calculate the vertical acceleration, velocity, and displacement trajectories of the sacrum. Similar to [9, 29], the jump was then split into the



**Table 1** Definition of kinematic and temporal parameters extracted from sacral displacement and velocity time history curves for each subject

Parameter	Definition
$t_{C1}$ (s)	Duration of C1
$t_{C2}$ (s)	Duration of C2
$t_P$ (s)	Duration of P
$t_j$ (s)	Duration of jump ( $t_{C1} + t_{C2} + t_P$ , not indicated in Fig. 2)
$d_j$ (m)	Maximum vertical displacement (not indicated in Fig. 2)
$d_C$ (m)	Vertical displacement at bottom of countermovement
$v_P$ (m/s)	Maximum vertical velocity
$v_C$ (m/s)	Minimum vertical velocity
$a_P$ (m/s <sup>2</sup> )	Average vertical acceleration during P
$a_{C1}$ (m/s <sup>2</sup> )	Average vertical acceleration during C1
$a_{C2}$ (m/s <sup>2</sup> )	Average vertical acceleration during C2

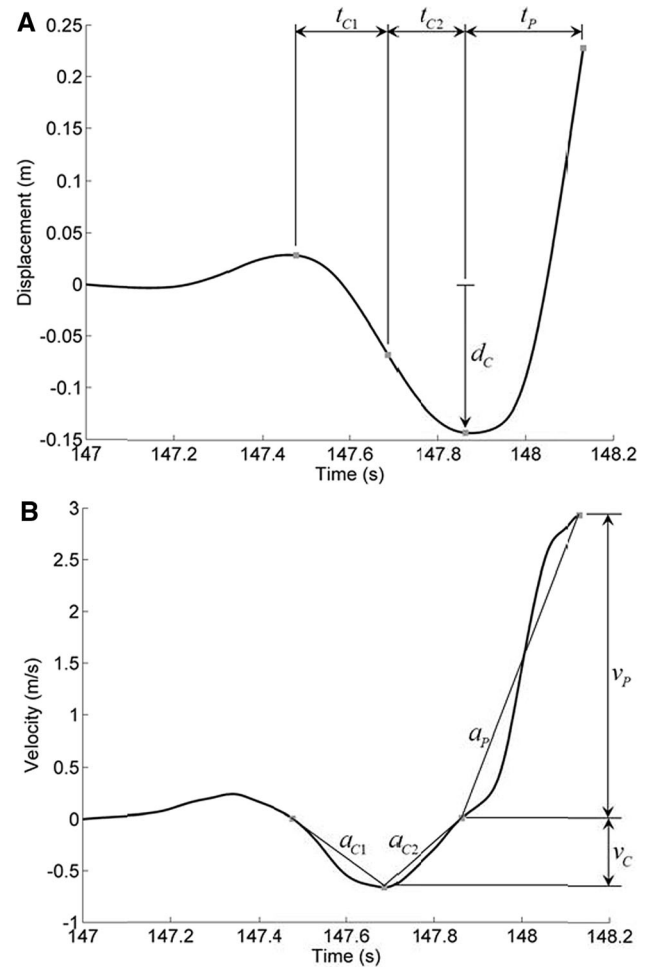
following phases: (1) start of countermovement (from initiation of countermovement to minimum vertical velocity, C1); (2) end of countermovement or braking (from minimum vertical velocity to bottom of countermovement, C2), and (3) propulsive (from bottom of countermovement to maximum vertical velocity, P). Kinematic and temporal parameters describing these three phases, defined in Table 1 and indicated in Fig. 2, were then extracted for further analysis.

#### 2.4.2 Statistical testing

The aforementioned sacral kinematic parameters were extracted from the four jumps completed in the unloaded, loaded fresh, and loaded fatigued conditions for each subject and averaged, yielding a single value of each sacral kinematic parameter, for each subject, for each condition. Statistically significant mean differences across conditions were established with paired-sample *t* tests ( $\alpha = 0.05$ ).

Multiple unadjusted linear models were used to examine the associations between jump height and the sacral kinematic and temporal parameters, regressing jump height on each of the parameters for each of the subject conditions (i.e., unloaded, loaded fresh, and loaded fatigued). If more than one significant association was identified, jump height was regressed on all of the significant parameters to control for shared variance and the resulting linear models were reported.

To examine the associations between change in jump height and change in the sacral kinematic and temporal parameters across conditions, the regressor method was used within a linear regression framework. We identified candidate significant associations by regressing jump height in the second condition (i.e., loaded or fatigued) on jump height in the first condition (i.e., unloaded or loaded

**Fig. 2** Kinematic and temporal parameters extracted from the sacral vertical displacement (a) and velocity (b) time histories for a sample jump

fresh) and changes in each of the parameters across conditions. When multiple significant associations were identified, jump height in the second condition was regressed on jump height in the first condition and changes in each of the significant parameters to control for shared variance. The resulting linear models are reported. We used the regressor method instead of directly modeling change in jump height to avoid known limitations associated with change modeling [30].

## 3 Results

### 3.1 Validity of the IMU-based method for estimating sacral kinematics

The acceleration, velocity, and displacement calculated from IMU (gray) and MOCAP (black) data are plotted against time during a representative countermovement

jump in Fig. 3a–c, respectively. The approximate flight phase of the jump is highlighted in these figures to foster interpretation. The agreement between the IMU and MOCAP-derived kinematic trajectories is further confirmed by the correlation plots for this representative jump presented in Fig. 4a–c. If the kinematics derived from IMU and MOCAP were identical, the cloud of points in each of the subplots would collapse to the black line which has unit slope and zero intercept.

To quantify the agreement between IMU and MOCAP estimates of the sacral kinematic trajectories we consider the mean and standard deviation (SD) of the difference between estimates of vertical acceleration, velocity, and displacement. For the jump highlighted in Figs. 3 and 4, the mean (SD) of the difference between IMU and MOCAP-derived acceleration, velocity, and displacement are 0.08 (0.94) m/s<sup>2</sup>, 0.01 (0.02) m/s, and −0.01 (0.01) m, respectively. For each of the correlation plots presented in Fig. 4, we fit a line to the cloud of points which should have slope and  $R^2$  equal to 1. In this case, the slope ( $R^2$ ) for the acceleration, velocity, and displacement are 0.99 (0.98), 1.00 (0.99), and 1.02 (0.99), respectively. The results of this example trial provide context for the summary results from all of the jumps considered ( $n = 252$ ) in Table 2. Reported in Table 2 are the mean (SD) of the mean difference, SD of the difference, intercept, slope, and  $R^2$  for all jumps analyzed.

The results presented in Table 2 establish the validity of the methodology for estimating sacral kinematic trajectories during vertical jumping. However, in vertical jump tests, practitioners often focus on maximum metrics including jump height (i.e., [4, 13, 31]) and maximum vertical velocity (i.e., [11]). To assess the validity of the IMU-based predictions of these metrics, we first consider Bland–Altman and correlation plots for jump height (Fig. 5a, b, respectively) and maximum vertical velocity (Fig. 6a, b, respectively). Bland–Altman plots provide a means for visualizing how the difference between IMU and MOCAP estimates (y axis) relates to the average of the two estimates (x axis). Three horizontal black lines indicate the mean and  $\pm 1.96$  SD of the difference between the estimates, this range is known as the Bland–Altman limits of agreement. As above, the correlation plot consists of the IMU estimates on the y axis and MOCAP estimates on the x axis with a black line with unit slope and zero intercept added for reference. Both plots provide a visual way to assess the agreement between IMU and MOCAP estimates for these established metrics of jumping performance.

To further quantify the agreement between IMU and MOCAP estimates of jump height, maximum vertical velocity ( $V_{MAX}$ ), and maximum vertical acceleration ( $A_{MAX}$ ), we report the mean and SD of the difference

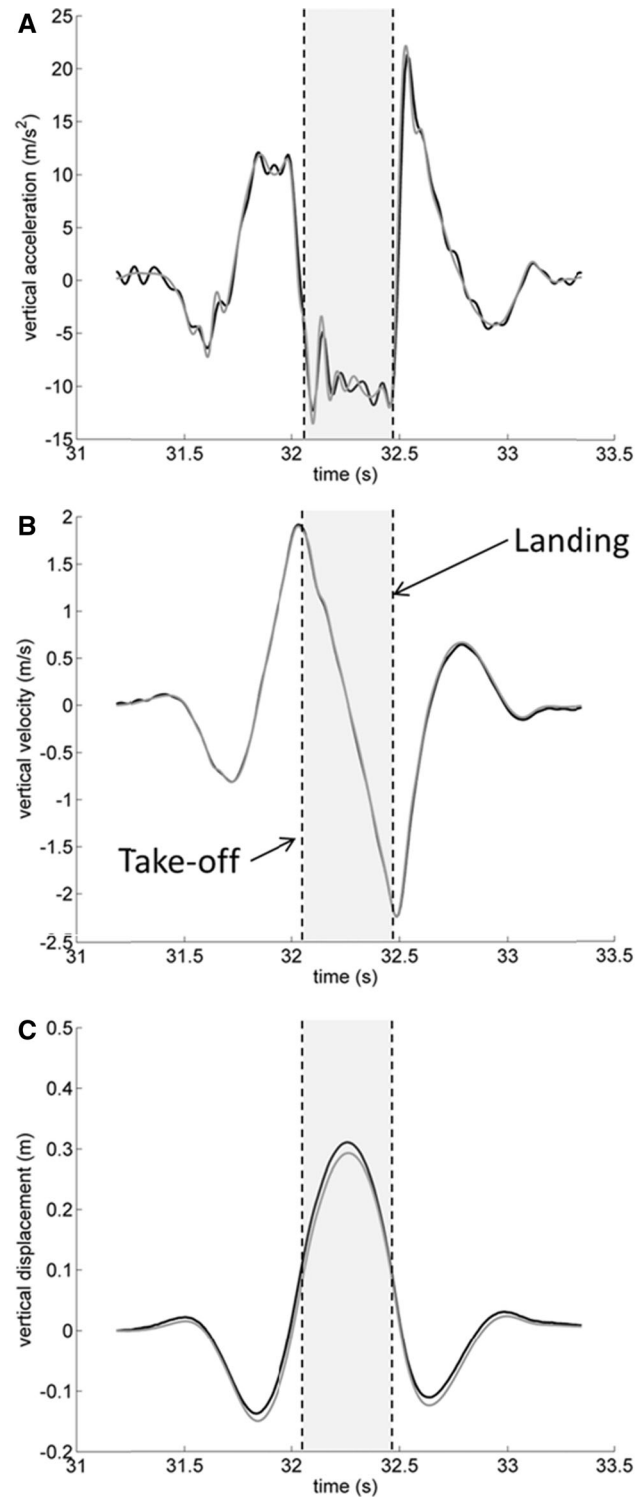


**Fig. 3** Vertical acceleration (a), velocity (b), and displacement (c) of the sacrum as calculated from IMU (gray) and MOCAP (black) data during a representative countermovement jump. The flight phase of the jump is highlighted for reference

between estimates from each motion sensing modality as well as the intercept, slope, and  $R^2$  of best-fit lines to correlation plot data in Table 3.

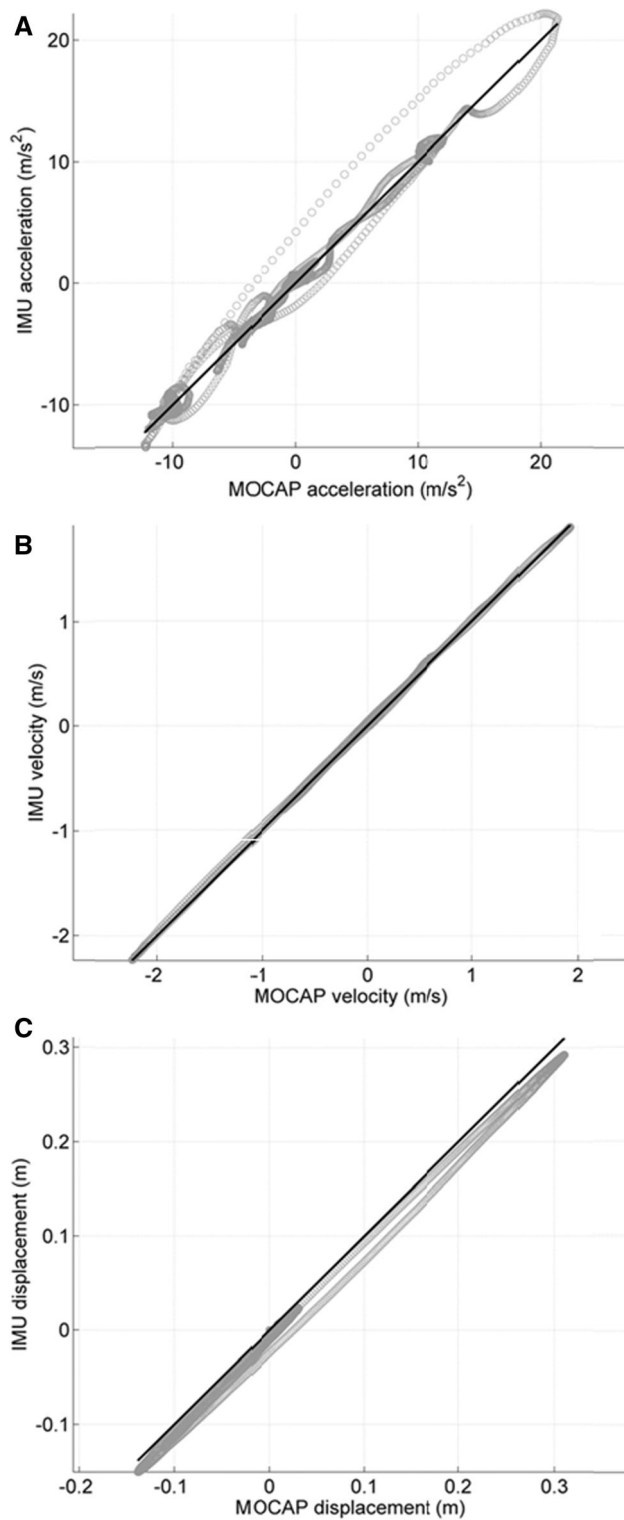


**Fig. 4** Correlation plots (IMU vs. MOCAP) for the vertical acceleration (a), velocity (b), and displacement (c) of the sacrum during a representative jump

To establish concurrent validity of the proposed IMU-based method to detect changes in sacral kinematics due to changes in load carriage conditions, we present box plots of

jump height,  $V_{MAX}$ , and  $A_{MAX}$  as estimated from IMU and MOCAP data in each load condition, in Fig. 7. Paired-sample  $t$  tests were used to test for significant differences in each metric for each motion sensing modality across condition. Both sensing modalities identify significant differences in jump height (IMU:  $t = -10.53$ ,  $p < 0.0001$ , MOCAP:  $t = -10.08$ ,  $p < 0.0001$ ), maximum vertical velocity (IMU:  $t = -11.24$ ,  $p < 0.0001$ , MOCAP:  $t = -10.36$ ,  $p < 0.0001$ ), and maximum vertical acceleration (IMU:  $t = -10.49$ ,  $p < 0.0001$ , MOCAP:  $t = -9.68$ ,  $p < 0.0001$ ) due to subject load carriage.

### 3.2 Effect of parameters on jump height

During the performance task, subjects completed four CMJs in an unloaded condition, four in a loaded fresh condition, and then, after completing an average (SD) of 5.5 (1.6) loaded bouts of the course, four CMJs in a loaded fatigued condition. During each set of jumps, segments of the body including the feet, shanks, thighs, and torso, are accelerated (thanks to highly coordinated contraction of muscles throughout the kinematic chain) to relatively high angular rates which act to straighten the body and propel the subject upwards. These segmental contributions yield the sacral kinematic trajectories and associated kinematic and temporal parameters described in Fig. 2 and Table 1. In the unloaded and loaded fresh conditions, only maximum vertical velocity ( $v_p$ ) was significantly associated with jump height ( $d_j$ ). In both cases, higher  $v_p$  was associated with higher jump height. Model results, including the coefficient of variation of the model ( $R^2$ ), and the coefficient ( $\beta$ ), standard error,  $t$  score ( $t$ ), and  $p$  value ( $p$ ) for each parameter, are reported for the unloaded and loaded fresh conditions in Tables 4 and 5, respectively.

In the loaded fatigued condition, unadjusted linear models in each parameter yielded significant associations between jump height and maximum vertical velocity, average vertical acceleration during the propulsive phase ( $a_p$ ), and depth of the countermovement ( $d_c$ ). These parameters were then used as regressors in an adjusted model to control for any shared variance. In the adjusted model, all three associations remained significant. As indicated by the model coefficients ( $\beta$ ) in Table 6, while holding the other parameters fixed, higher  $v_p$  and  $d_c$  (i.e., not dropping as far during the countermovement), and lower  $a_p$  are associated with higher jump height.

### 3.3 Changes in parameters across load and fatigue

The associations reported in Tables 4, 5 and 6 identify which kinematic and temporal parameters are indicative of the strategy used to maximize performance in the CMJ within each condition (unloaded, loaded fresh, loaded

**Table 2** Mean (standard deviation) of the mean and standard deviation (SD) of the difference between IMU and MOCAP estimates of sacral kinematics as well as the intercept, slope, and  $R^2$  of best-fit lines to the correlation plot data for all ( $n = 252$ ) trials

Variable	Mean	SD	Intercept	Slope	$R^2$
$a$ ( $\text{m/s}^2$ )	0.024 (0.088)	1.828 (0.560)	0.024 (0.088)	0.960 (0.033)	0.930 (0.037)
$v$ ( $\text{m/s}$ )	0.023 (0.026)	0.053 (0.049)	0.023 (0.026)	0.999 (0.014)	0.993 (0.017)
$d$ (m)	0.003 (0.032)	0.020 (0.024)	0.003 (0.031)	0.969 (0.083)	0.977 (0.046)

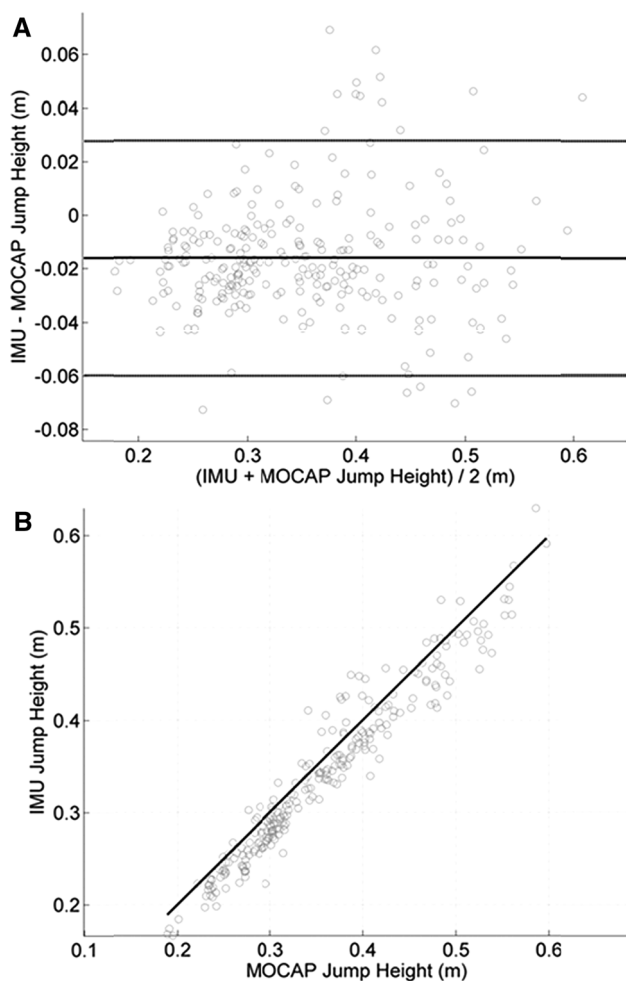


**Fig. 5** Bland–Altman (a) and correlation (b) plots establish agreement between IMU and MOCAP estimates of jump height. Bland–Altman plot includes *lines* corresponding to the mean and  $\pm 1.96$  SD of the difference between estimates. Correlation plot includes a *black line* with unit slope and zero intercept

fatigued) by the subject population considered in this study. As these parameters have not been investigated in detail in the literature, it is also illustrative to consider how load and fatigue affect changes in our kinematic and temporal metrics. Table 7 reports the average change in each of these parameters across load ( $\Delta_L = \text{loaded} - \text{unloaded}$ ) and fatigue ( $\Delta_F = \text{fatigued} - \text{fresh}$ ) along with the  $t$  statistic and  $p$  value testing the null hypothesis that this

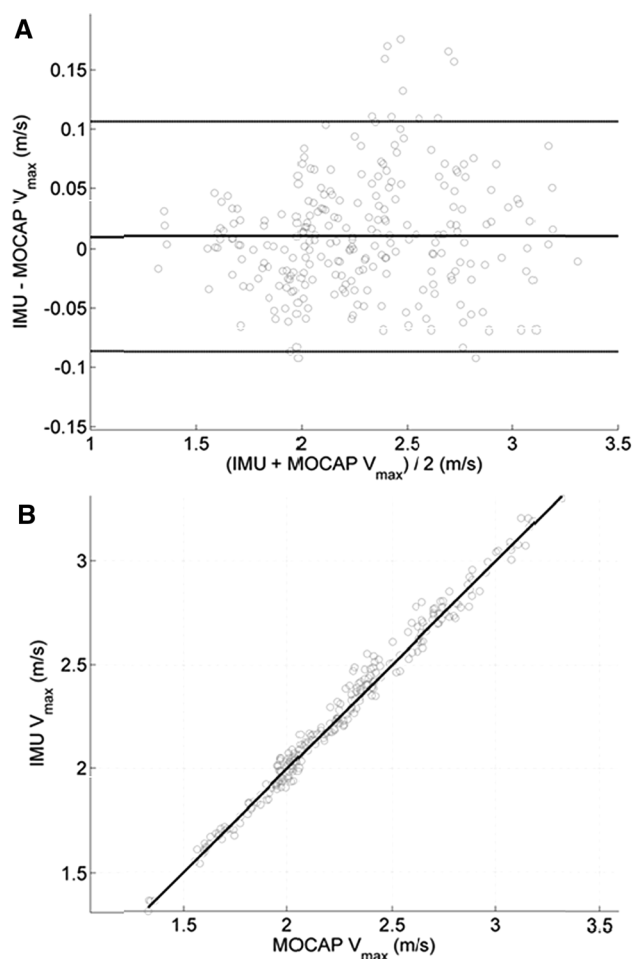


**Fig. 6** Bland–Altman (a) and correlation (b) plots establish agreement between IMU and MOCAP estimates of maximum vertical velocity. Bland–Altman plot includes *lines* corresponding to the mean and  $\pm 1.96$  SD of the difference between estimates. Correlation plot includes a *black line* with unit slope and zero intercept

sample is from a population with no difference across condition.

### 3.4 Effect of changes in parameters on changes in jump height across load and fatigue

Across load, unadjusted linear models of change in jump height by change in each parameter yielded significant associations with change in the depth of the



**Table 3** Mean and standard deviation of the difference between IMU and MOCAP estimates of maximum vertical acceleration, maximum vertical velocity, and jump height as well as the intercept, slope, and  $R^2$  of best-fit lines to the correlation plot data for all ( $n = 252$ ) trials

Variable	Mean	SD	Intercept	Slope	$R^2$
$A_{\text{MAX}}$ ( $\text{m/s}^2$ )	-0.282	0.742	-0.077	0.986	0.972
$V_{\text{MAX}}$ ( $\text{m/s}$ )	0.010	0.049	-0.006	1.007	0.986
Jump height (m)	-0.016	0.022	-0.012	0.990	0.940

countermovement ( $\Delta d_C$ ) and change in the duration of the propulsive phases of the jump ( $\Delta t_P$ ). As before, these parameters were then used as regressors in an adjusted model and both associations remained significant. As indicated by the model coefficients ( $\beta$ ) in Table 8, while controlling for jump height in the unloaded condition and holding the other parameter fixed, positive changes in  $d_C$  (i.e., not dropping as far during the countermovement when loaded) and  $t_P$  (i.e., increasing the duration of the propulsive phase when loaded) across load are associated with higher jump height in the loaded fresh condition.

Across fatigue, unadjusted linear models of change in jump height by change in each parameter yielded significant associations with change in the depth of the countermovement ( $\Delta d_C$ ) and change in the maximum vertical velocity ( $\Delta v_P$ ). As before, these parameters were then used as regressors in an adjusted model and both associations remained significant. As indicated by the model coefficients ( $\beta$ ) in Table 9, while controlling for jump height in the loaded fresh condition and holding the other parameter fixed, positive changes in  $\Delta d_C$  (i.e., not dropping as far during the countermovement when fatigued) and  $\Delta v_P$  (i.e., increasing the maximum vertical velocity when fatigued) across fatigue are associated with higher jump height in the loaded fatigued condition.

#### 4 Discussion

An IMU-based method for estimating sacral kinematics during vertical jumping is introduced herein and its accuracy is established via a detailed comparison to MOCAP. This method improves upon existing methods because it provides estimates of sacral kinematic trajectories in addition to simply jump height. In this section, we discuss the agreement between IMU and MOCAP estimates of sacral kinematic trajectories, jump height and maximum vertical velocity (common jump performance metrics), and changes that occur across load to establish the validity of our methodology. The proposed technique is then used in an investigation of changes in sacral kinematic parameters during vertical jumping across load and fatigue, which has not previously been investigated using an IMU-based

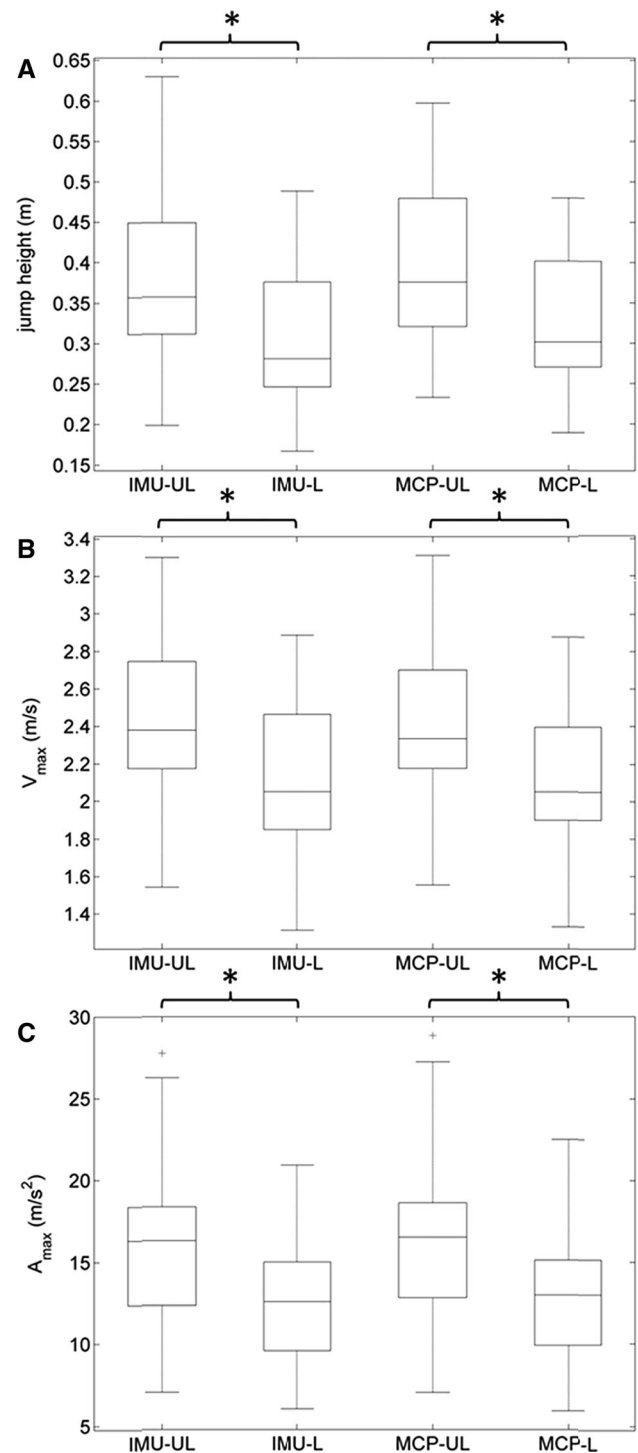


**Fig. 7** Box plots of jump height (a), maximum vertical velocity (b), and maximum vertical acceleration (c) across load conditions as estimated from IMU and MOCAP (MCP) data. L (UL) signifies loaded (unloaded) conditions. Significant difference in metrics between load conditions noted with an asterisk

approach. We compare significant associations between parameters extracted from sacral kinematic trajectories and jump height within each condition, discuss changes in these

**Table 4** Linear model of  $d_j$  as predicted by  $v_P$  in the unloaded condition

Parameter	$\beta$ (std. err)	$t$	$p$
$v_P$ (m/s)	0.26 (0.04)	6.64	$<0.001^+$
$R^2 = 0.70$			
$^+ p < 0.01$			

**Table 5** Linear model of  $d_j$  as predicted by  $v_P$  in the loaded fresh condition

Parameter	$\beta$ (std. err)	$t$	$p$
$v_P$ (m/s)	0.23 (0.04)	6.23	$<0.001^+$
$R^2 = 0.67$			
$^+ p < 0.01$			

**Table 6** Adjusted linear model of  $d_j$  as predicted by  $v_P$ ,  $a_P$ , and  $d_C$  in the loaded fatigued testing condition for all subjects

Parameter	$\beta$ (std. err)	$t$	$p$
$v_P$ (m/s)	0.30 (0.02)	15.00	$<0.001^+$
$a_P$ (m/s <sup>2</sup> )	-0.01 ( $<0.01$ )	-2.60	0.019*
$d_C$ (m)	0.95 (0.10)	9.40	$<0.001^+$
Adjusted $R^2 = 0.96$			
$^+ p < 0.01$ , * $p < 0.05$			

**Table 7** Mean difference in sacral kinematic metrics across load ( $\Delta_L$  = loaded – unloaded) and fatigue ( $\Delta_F$  = fatigued – fresh) are reported along with the  $t$  scores and  $p$  values of paired-sample  $t$  tests comparing metrics across conditions

Parameter	$\Delta_L$	$t_L$	$p_L$	$\Delta_F$	$t_F$	$p_F$
$d_j$ (m)	-0.08	-3.70	0.001 <sup>+</sup>	-0.11	-5.26	$<0.001^+$
$v_P$ (m/s)	-0.24	-4.25	$<0.001^+$	-0.22	-3.22	0.004 <sup>+</sup>
$a_P$ (m/s <sup>2</sup> )	-1.90	-3.46	0.003 <sup>+</sup>	1.39	2.36	0.03*
$d_C$ (m)	0.01	0.81	0.430	0.05	3.48	0.002 <sup>+</sup>
$v_C$ (m/s)	0.06	1.84	0.080	0.19	4.64	$<0.001^+$
$a_{C1}$ (m/s <sup>2</sup> )	0.34	0.87	0.400	0.45	1.15	0.26
$a_{C2}$ (m/s <sup>2</sup> )	-0.37	-0.62	0.540	-0.06	-0.15	0.88
$t_{C1}$ (s)	-0.01	-0.09	0.930	-0.07	-0.88	0.39
$t_{C2}$ (s)	$<0.01$	0.67	0.510	-0.03	-3.73	0.001 <sup>+</sup>
$t_P$ (s)	0.02	1.94	0.060	-0.06	-4.41	$<0.001^+$
$t_j$ (s)	0.01	0.14	0.890	-0.15	-1.94	0.07

<sup>+</sup>  $p < 0.01$ , \*  $p < 0.05$

parameters across conditions, and explore significant associations between these changes and changes in jump height across conditions to accelerate the adoption of this technology for CMJ training and related purposes.

**Table 8** Adjusted linear model of  $d_j$  in the loaded fresh condition as predicted by  $d_j$  in the unloaded condition and changes in  $d_C$  and  $t_P$ 

Parameter	$\beta$ (std. err)	$t$	$p$
$d_j$ (m)	0.60 (0.06)	10.34	$<0.001^+$
$\Delta d_C$ (m)	0.65 (0.14)	4.71	$<0.001^+$
$\Delta t_P$ (s)	1.09 (0.19)	5.73	$<0.001^+$

Adjusted  $R^2 = 0.85$

<sup>+</sup>  $p < 0.01$

**Table 9** Adjusted linear models of  $d_j$  in the loaded fatigued condition as predicted by  $d_j$  in the loaded fresh condition and changes in  $d_C$  and  $v_P$ 

Parameter	$\beta$ (std. err)	$t$	$p$
$d_j$ (m)	0.67 (0.12)	5.35	$<0.001^+$
$\Delta d_C$ (m)	0.85 (0.15)	5.53	$<0.001^+$
$\Delta v_P$ (m/s)	0.19 (0.03)	5.87	$<0.001^+$

Adjusted  $R^2 = 0.81$

<sup>+</sup>  $p < 0.01$

#### 4.1 Validity of IMU-based methodology for estimating sacral kinematics

The validity of inertial sensor-based methodologies for estimating vertical jump height, flight time, and maximum vertical velocity have been investigated in detail in the literature (i.e., [11, 13, 17, 18, 21, 22]). We build upon this existing work by presenting a methodology that utilizes a single, sacrum-mounted IMU for calculating the complete time histories of vertical acceleration, velocity, and displacement during the CMJ. The results presented in Table 2 demonstrate that this method reproduces MOCAP-estimated vertical acceleration, velocity, and displacement trajectories to within average mean (SD) differences of 0.024 (1.828) m/s<sup>2</sup>, 0.023 (0.053) m/s, and 0.003 (0.020) m, respectively. This excellent agreement is further supported by the regression analysis results presented in Table 2, including the mean slope ( $R^2$ ) values for acceleration, velocity, and displacement of 0.960 (0.930), 0.999 (0.993), and 0.969 (0.977), respectively. The slope values suggest that, on average, the IMU underestimates changes in acceleration by 4 %, velocity by  $<0.1$  %, and displacement by 3 % relative to the MOCAP-estimated values. The  $R^2$  (coefficient of variation) values suggest that, on average, the IMU estimates explain 93, 99, and 98 % of the variation in the MOCAP estimates of acceleration, velocity, and displacement, respectively. The modest remaining differences are likely due to a number of small factors including misalignment of the MOCAP and IMU vertical directions,

difference between MOCAP and IMU sacral position, small remaining drift errors in the IMU velocity and displacement, and noise amplification in MOCAP acceleration and velocity due to differentiation of marker position data.

The excellent agreement between IMU and MOCAP kinematic trajectories extends to two of the kinematic parameters typically used to assess jump performance; namely, jump height and maximum vertical velocity ( $V_{MAX}$ ). The Bland–Altman and correlation plots of Figs. 5 and 6 suggest that the agreement between IMU and MOCAP predictions of jump height (Fig. 5) and  $V_{MAX}$  (Fig. 6) is homoscedastic, and remains quite close across the range of jumps tested. Specifically, the results presented in Table 3 demonstrate that the proposed methodology reproduces MOCAP jump height and  $V_{MAX}$  to within a mean (SD) difference of  $-0.016$  ( $0.022$ ) m and  $0.010$  ( $0.049$ ) m/s, respectively. The regression analysis results reported in Table 3 (i.e., intercept, slope, and  $R^2$ ) confirm this agreement. For jump height specifically, the intercept suggests that the proposed methodology systematically underestimates MOCAP jump height by  $0.012$  m ( $<5$  % of the mean jump height from MOCAP). The slope and  $R^2$  values suggest that despite this systematic bias, the methodology accurately quantifies differences in jump height to within 1 % of the MOCAP estimates and that 94 % of the variation in the MOCAP jump height is explained by the IMU jump height estimate. Similarly, for  $V_{MAX}$  the intercept suggests that the IMU-based methodology slightly underestimates the MOCAP estimate by  $0.006$  m/s ( $<0.3$  % of mean  $V_{MAX}$  from MOCAP). The slope and  $R^2$  values again suggest that this methodology detects differences in  $V_{MAX}$  to within 0.7 % of the MOCAP estimates and that 99 % of the variation in the MOCAP estimates of  $V_{MAX}$  is explained by the IMU estimates.

In Table 3, we also establish the accuracy of a third potential jump height performance metric:  $A_{MAX}$ . Assuming the device's accelerometer is collocated with the subject mass center, as is nearly the case when indexed against the sacrum, this value (maximum vertical acceleration) is necessarily proportional to the maximum vertical ground reaction force generated by the subject during the jump, and could therefore be a useful performance metric. The proposed methodology reproduces MOCAP  $A_{MAX}$  to within a mean (SD) difference of  $-0.282$  ( $0.742$ ) m/s<sup>2</sup>. The regression analysis results suggest that the IMU-based method systematically underestimates  $A_{MAX}$  by only  $0.077$  m/s<sup>2</sup> ( $<0.6$  %) as compared to MOCAP. It also detects differences in  $A_{MAX}$  to within 1.4 % of the MOCAP estimates, and 97 % of the variation in the MOCAP estimates of  $A_{MAX}$  is explained by the IMU estimates.

Finally, to demonstrate the concurrent validity of the proposed IMU methodology, we report in Fig. 7 the observed difference in jump height,  $V_{MAX}$ , and  $A_{MAX}$  due to

the addition of an 18 kg load. The difference in each parameter across load was statistically significant based on data from each motion sensing modality. This finding enforces the validation results above and further establishes that this technology yields sacral kinematics with sufficient precision to accurately track changes in key kinematic metrics during vertical jumping. Doing so could impact multiple applications, including screening for susceptibility to lower body injuries and athletic performance, tracking recovery from an injury, and tracking progress during a training season.

## 4.2 Effect of parameters on jump height

To further these advances, one needs to establish candidate kinematic metrics that predict success. Measuring and reporting jump height is imperative, but we seek to identify the underlying kinematical metrics that most influence jump height and thereby reveal fundamental limitations to jump performance. To that end, we parameterized sacral kinematics by the variables listed in Table 1, and identified the parameters that were significantly associated with jump height in the unloaded, loaded fresh, and loaded fatigued testing conditions. For the unloaded and loaded fresh conditions, only  $v_P$  was significantly associated with jump height. Considering simple projectile motion of the subject while airborne, jump height is entirely dependent on flight time, which is, in turn, solely dependent on take-off velocity. Maximum vertical velocity may not always be the take-off velocity, but it has served as a proxy in other studies (i.e., [11]). The fact that the only significant predictor of jump height is  $v_P$  suggests that our subject population (untrained in the CMJ) utilizes a variety of strategies to achieve their maximum CMJ height. In contrast, in the loaded fatigued condition, subjects seem to regress towards a common jumping strategy where higher jump heights are associated with higher  $v_P$ , lower  $a_P$ , and a shallower countermovement. This three-predictor model fits the data well (adjusted  $R^2$  of 0.96), explaining 96 % of the variance in jump height. One possible explanation for the association between a shallower countermovement and higher jump height could be a change in CMJ strategy adopted by subjects in response to fatigue-induced changes in the stretch–shortening cycle (SSC) of their musculature. Specifically, in non-fatigued muscle the SSC converts stretching induced during the transition between the countermovement and propulsive phases of the jump into heightened contractile forces. However, in the presence of muscular fatigue the SSC loses effectiveness, and these force gains are no longer observed [32]. As the benefits of the countermovement are diminished, subjects could have chosen to alter their jumping strategy to avoid the added costs. Namely, a shallower countermovement minimizes

the distance a subject moves their center of mass which could be advantageous in a loaded fatigued condition where any additional required work could prevent successful execution of the jump. The association between lower  $a_P$  and higher jump heights is curious, and could possibly be due to an observed association between  $a_P$  and  $t_P$ . Specifically, subjects who had lower  $a_P$  also exhibited longer  $t_P$  yielding a larger impulse (impulse  $\propto a_P \cdot t_P$ ) and therefore larger  $v_P$  and jump height [33].

#### 4.3 Changes in parameters across load and fatigue

For this technology to be used to monitor and track changes in the kinematics of the CMJ across load and fatigue conditions, we need to establish which of the kinematic parameters exhibit changes. To this end, Table 7 reports mean changes in each of the kinematic and temporal variables across load and fatigue for all subjects. Only jump height ( $-0.08$  m),  $v_P$  ( $-0.24$  m/s), and  $a_P$  ( $-1.90$  m/s<sup>2</sup>) exhibit statistically significant changes across load, and all three parameters decreased as expected. These quantities, when combined with timing variables are directly linked (i.e.,  $v_P = a_P \cdot t_P$ ), so decreases in  $v_P$  and  $a_P$  are expected to accompany the decrease in jump height associated with added load. Using a force plate, Vaverka et al. [29] found that jump height decreases linearly by an average of 4 cm for every additional 10 % body weight loading. Similarly, in this study we find that jump height decreases by 8 cm in response to the 18 kg load ( $\sim 24$  % body weight) applied to the subjects. The duration of the end of countermovement ( $t_{C2}$ ) and propulsive ( $t_P$ ) phases each increased, although not significantly, which also aligns with the findings of [29]. The similarities between these results and those obtained using the force plate methodology [29] further validates the proposed IMU-based approach which adds the significant advantage of easy use outside the laboratory.

Across fatigue, jump height ( $-0.11$  m),  $v_P$  ( $-0.24$  m/s),  $a_P$  ( $-1.90$  m/s<sup>2</sup>),  $d_C$  ( $0.05$  m),  $v_C$  ( $0.19$  m/s),  $t_{C2}$  ( $-0.03$  s), and  $t_P$  ( $-0.06$  s) all exhibit significant changes. As with the changes across load, decreases in  $v_P$  and  $a_P$  are expected to accompany the decrease in jump height associated with fatigue. In [9], fatigue of knee extensor muscles caused a 4.6 cm decrease in CMJ height. Similarly, in [34] a soccer match yielded a 4.4 cm decrease in CMJ height. In [8], performing repeated CMJs until fatigue yielded a 9.8 cm decrease in CMJ height after an average of 30.6 continuous jumps with arms crossed across the chest. Herein CMJ height decreases by an average of 11 cm across fatigue. The larger decrease in jump height could be due to several factors including the inclusion of an 18 kg load during the fatiguing protocol which could introduce a more dramatic fatigue affect than shown in other studies. Moreover, the

obstacle course used in this study was designed to induce fatigue across multiple (lower and upper limb) muscle groups which runs counter to [9], where only the knee extensor muscles were fatigued. This whole-body fatigue could also be responsible for the larger decrease in CMJ height in this study. The depth of the countermovement became shallower by 5 cm across fatigue, which is similar to findings in [9] where fatigue of the knee extensor muscles resulted in shallower countermovements as well. As noted earlier, this potentially indicates a change in strategy as a result of changes in the stretch-shortening properties of the muscles used for jumping and/or because a shallower countermovement ensures that the CMJ can still be completed successfully. Finally, the duration of the braking ( $t_{C2}$ ) and propulsive ( $t_P$ ) phases decreased by 0.03 and 0.06 s, respectively. In contrast, the duration of the propulsive phase increased by 0.03 s in [8]. The difference is likely due to changes in jumping strategy that result from subjects being fatigued under load (as opposed to just fatigued) as discussed earlier.

#### 4.4 Effect of changes in parameters on changes in jump height across load and fatigue

As evidenced by the results in Table 7, while all of the parameters exhibit mean differences across load and fatigue, only some are common between subjects (i.e., statistically significant). To support CMJ training, it is important to investigate which of these changes exhibit a significant association with the changes in jump height that occur across conditions. Such changes reveal which technique modifications optimize performance under these naturalistic conditions.

The results in Table 8 demonstrate that changes in jump height across load are significantly associated with changes in countermovement depth ( $\Delta d_C$ ) and duration of the propulsive ( $\Delta t_P$ ) phase. This two-parameter model explains 85 % of the variance in the change in jump height. Specifically, holding  $\Delta t_P$  constant, if a subject increases  $\Delta d_C$  by 1 cm (i.e., reduces the loaded countermovement by 1 cm), they could increase their loaded jump height by 0.65 cm. Similarly, holding  $\Delta d_C$  constant, if a subject increases  $\Delta t_P$  by 0.01 s (i.e., increase the duration of the loaded propulsive phase by 0.01 s), they could increase their loaded jump height by 1.09 cm. These influences seem to counter each other. Namely, if the depth of the countermovement is reduced then the subject needs higher acceleration during the propulsive phase to achieve the same take-off velocity and must do so in less time hence decrease the duration of the propulsive phase and  $\Delta t_P$  as well. This dichotomy suggests that to increase loaded jump height (minimize the decrease in jump height associated with load), subjects should focus on either decreasing the



depth of their countermovement or increasing the duration of their propulsive phase, as one strategy precludes the other. Further work across multiple loaded states may afford greater insights here.

Table 9 demonstrates that changes in jump height across fatigue are significantly associated with changes in countermovement depth ( $\Delta d_C$ ) and maximum propulsive velocity ( $\Delta v_P$ ). In this case, the two-parameter model explains 81 % of the variance in the change in jump height. In similar fashion to the load comparison, holding the other parameter constant, if a subject increases their  $\Delta d_C$  by 1 cm, they could increase their fatigued jump height by 0.85 cm. As suggested before, this association is likely caused by a change in CMJ strategy to avoid reliance on the stretch-shortening cycle for force production which has been shown to lose effectiveness when muscles are fatigued [32]. Holding  $\Delta d_C$  fixed, if a subject increases their  $\Delta v_P$  (i.e., does not reduce  $v_P$  when fatigued), then they can increase their CMJ height. Unlike in the loaded condition, subjects may potentially exploit both strategies simultaneously; namely decreasing the depth of the countermovement while maximizing  $v_P$  in the loaded fatigued condition. Since the duration of the propulsive phase is constrained by the depth of the countermovement, this could be accomplished by holding  $t_P$  fixed and increasing the average acceleration during the propulsive phase. In sum, for subjects to increase their CMJ height in a loaded and fatigued state, it appears the focus should be on maintaining their non-fatigued maximum vertical velocity while decreasing the depth of their countermovement.

## 5 Conclusion

Results from 252 jumps (across 14 subjects), reveal that the IMU-based method reproduces the vertical acceleration, velocity, and displacement trajectories of the sacrum measured by MOCAP to within a mean (SD) difference of 0.024 (0.088) m/s<sup>2</sup>, 0.023 (0.026) m/s, and 0.003 (0.032) m, respectively. The method also quantifies differences in jump height to within 1 % and differences in  $V_{MAX}$  to within 0.7 % of MOCAP estimates. The CMJ kinematics results reveal the method's ability to effectively discriminate key jump height kinematic parameters across explicit load and fatigue conditions. In so doing, it provides a platform for innovative biomechanically based performance screening and optimization in naturalistic environments. The utility of the method is further demonstrated in its ability to discriminate these metrics across a diverse subject population, which appear to naturally adopt a similarly diverse set of strategies to achieve maximal jump heights under normal conditions. In particular, the participants adopted multiple strategies to maximize jump height

in the unloaded and loaded fresh conditions, but converged to a common strategy when jumping fatigued and under load. Changes in kinematic parameters were evident across conditions, and several changes were significantly associated with changes in jump performance (i.e., height). These parameters include changes in the depth of the countermovement, duration of the propulsive phase and maximum propulsive velocity. Collectively, the results presented herein point toward the future use of this method in naturalistic environments and for multiple objectives including biomechanical performance assessment and tracking, fatigue assessment, and jump training.

**Acknowledgments** Funding for this study was provided by the US Army Natick Soldier Research, Development and Engineering Center—Contract # W911QY-13-C-0011. Thanks are due to Bryan Schlink for his help with the sacral kinematics validation.

## References

1. Innocenti B, Facchielli D, Torti S, Verza A (2006) Analysis of biomechanical quantities during a squat jump: evaluation of a performance index. *J Strength Cond Res Natl Strength Cond Assoc* 20(3):709–715
2. James LV, Dowling J (1993) Identification of kinetic and temporal factors related to vertical jump performance. *J Appl Biomech* 9:95–110
3. Häkkinen K (1991) Force production characteristics of leg extensor, trunk flexor and extensor muscles in male and female basketball players. *J Sports Med Phys Fit* 31(3):325–331
4. Harman EA, Rosenstein MT, Frykman PN, Rosenstein RM, Kraemer WJ (1991) Estimation of human power output from vertical jump. *J Strength Cond Res* 5(3):116–120
5. Rosendal L, Langberg H, Skov-Jensen A, Kjaer M (2003) Incidence of injury and physical performance adaptations during military training. *Clin J Sport Med Off J Can Acad Sport Med* 13(3):157–163
6. Paterno MV, Ford KR, Myer GD, Heyl R, Hewett TE (2007) Limb asymmetries in landing and jumping 2 years following anterior cruciate ligament reconstruction. *Clin J Sport Med* 17(4):258–262
7. Clanton TO, Matheny LM, Jarvis HC, Jeronimus AB (2012) Return to play in athletes following ankle injuries. *Sports Health Multidiscip Approach* 4(6):471–474. doi:10.1177/1941738112463347
8. Rodacki AL, Fowler NE, Bennett SJ (2001) Multi-segment coordination: fatigue effects. *Med Sci Sports Exerc* 33(7):1157–1167
9. Rodacki ALF, Fowler NE, Bennett SJ (2002) Vertical jump coordination: fatigue effects. *Med Sci Sports Exerc* 34(1):105–116
10. Leard JS, Cirillo MA, Katsnelson E, Kimiatek DA, Miller TW, Trebincevic K, Garbalosa JC (2007) Validity of two alternative systems for measuring vertical jump height. *J Strength Cond Res Natl Strength Cond Assoc* 21(4):1296–1299
11. de Villarreal ES-S, Garcia I, Paasuke M, Requena B, Requena F (2012) Reliability and validity of a wireless microelectromechanicals based system (Keimove[TM]) for measuring vertical jumping performance. *J Sports Sci Med* 11(1):115
12. Glatthorn JF, Gouge S, Nussbaumer S, Stauffacher S, Impelizzeri FM, Maffioletti NA (2011) Validity and reliability of Optojump photoelectric cells for estimating vertical jump height. *J Strength Cond Res Natl Strength Cond Assoc* 25(2):556–560

13. Castagna C, Ganzetti M, Ditroilo M, Giovannelli M, Rocchetti A, Manzi V (2013) Concurrent validity of vertical jump performance assessment systems. *J Strength Cond Res Natl Strength Cond Assoc* 27(3):761–768
14. Dias JA, Dal Pupo J, Reis DC, Borges L, Santos SG, Moro ARP, Borges NG Jr (2011) Validity of two methods for estimation of vertical jump height. *J Strength Cond Res Natl Strength Cond Assoc* 25(7):2034–2039
15. García-López J, Morante JC, Ogueta-Alday A, Rodríguez-Marroyo JA (2013) The type of mat (Contact vs. Photocell) affects vertical jump height estimated from flight time. *J Strength Cond Res Natl Strength Cond Assoc* 27(4):1162–1167
16. Isaacs LD (1998) Comparison of the Vertec and Just Jump systems for measuring height of vertical jump by young children. *Percept Mot Skills* 86(2):659–663
17. Nuzzo JL, Anning JH, Scharfenberg JM (2011) The reliability of three devices used for measuring vertical jump height. *J Strength Cond Res Natl Strength Cond Assoc* 25(9):2580–2590
18. Casartelli N, Müller R, Maffioletti NA (2010) Validity and reliability of the Myotest accelerometric system for the assessment of vertical jump height. *J Strength Cond Res* 24(11):3186–3193
19. Balsalobre-Fernández C, Tejero-González CM, del Campo-Vecino J, Bavaresco N (2014) The concurrent validity and reliability of a low-cost, high-speed camera-based method for measuring the flight time of vertical jumps. *J Strength Cond Res Natl Strength Cond Assoc* 28(2):528–533
20. Júnior B, Gomes N, Borges L, Dias JA, Wentz MD, da Mattos DJS, Petry R, Domenech SC (2011) Validity of a new contact mat system for evaluating vertical jump. *Mot Rev Educ Física* 17(1):26–32
21. Quagliarella L, Sasanelli N, Belgiovine G, Moretti L, Moretti B (2010) Evaluation of standing vertical jump by ankles acceleration measurement. *J Strength Cond Res Natl Strength Cond Assoc* 24(5):1229–1236
22. Dowling AV, Favre J, Andriacchi TP (2011) A wearable system to assess risk for anterior cruciate ligament injury during jump landing: measurements of temporal events, jump height, and sagittal plane kinematics. *J Biomech Eng* 133(7):071008
23. Picerno P, Camomilla V, Capranica L (2011) Countermovement jump performance assessment using a wearable 3D inertial measurement unit. *J Sports Sci* 29(2):139–146
24. McGinnis RS, Perkins NC (2012) A highly miniaturized, wireless inertial measurement unit for characterizing the dynamics of pitched baseballs and softballs. *Sensors* 12(9):11933–11945
25. King KW (2008) The design and application of wireless MEMS inertial measurement units for the measurement and analysis of golf swings. Ph.D., University of Michigan, Ann Arbor
26. Savage P (2000) Strapdown analytics. Strapdown Associates, Maple Plain
27. Titterton DH, Weston JL (2004) Strapdown inertial navigation technology, 2nd edn. Institution of Electrical Engineers, Stevenage
28. Borg G (1998) Borg's perceived exertion and pain scales, vol viii. Human Kinetics, Champaign
29. Vaverka F, Jakubsova Z, Jandacka D, Zahradnik D, Farana R, Uchytel J, Supej M, Vodcar J (2013) The influence of an additional load on time and force changes in the ground reaction force during the countermovement vertical jump. *J Hum Kinet* 38:191–200
30. Vickers AJ, Altman DG (2001) Analysing controlled trials with baseline and follow up measurements. *BMJ* 323(7321):1123–1124
31. Bosco C, Luhtanen P, Komi PV (1983) A simple method for measurement of mechanical power in jumping. *Eur J Appl Physiol* 50(2):273–282
32. Komi PV (2000) Stretch-shortening cycle: a powerful model to study normal and fatigued muscle. *J Biomech* 33(10):1197–1206
33. Kirby TJ, McBride JM, Haines TL, Dayne AM (2011) Relative net vertical impulse determines jumping performance. *J Appl Biomech* 27(3):207–214
34. Andersson H, Raastad T, Nilsson J, Paulsen G, Garthe I, Kadi F (2008) Neuromuscular fatigue and recovery in elite female soccer: effects of active recovery. *Med Sci Sports Exerc* 40(2):372–380